Supplementary Materials

A novel surface passivation method of pyrite within rocks in water-filled mining tunnels to mitigate acid mine drainage at its source

Lijun Fan, Tiancheng Han, Yixuan Yang, Xianxing Huang, Tao Zhu, Weiwei Zhai, Daoyong Zhang, Xiangliang Pan*

Key Laboratory of Microbial Technology for Industrial Pollution Control of Zhejiang Province, College of Environment, Zhejiang University of Technology, Hangzhou, China

**Corresponding author: Xiangliang Pan*

Tel: (86) 0571-88320249; Fax: (86) 0571-88320249

Address: No. 18, Chaowang Road, Hangzhou City, Zhejiang Province, China

E-mail: panxl@zjut.edu.cn

Summary:

Figure S1. The XRD spectrum of the pyrite sample.

Figure S2. SEM images of uncoated pyrite (a, c) and TA-5.0 PEG coated pyrite (b, d) before and after a 21-day chemical leaching experiment.

Figure S3. XPS full spectra of uncoated, TA, and TA-5.0 PEG coated pyrite.

Figure S4. XPS devolution spectra of S 2p of uncoated, TA, and TA-5.0 PEG coated pyrite.

Table S1. XPS fitting of C 1s, O 1s, Fe 2p, and S 2p of uncoated pyrite, TA, and TA-5.0 PEG coated pyrite.

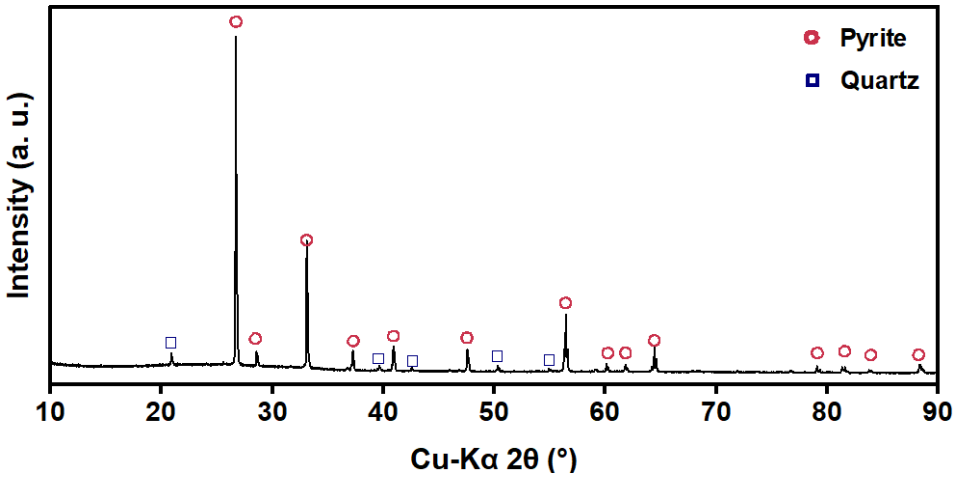


Figure S1. The XRD spectrum of the pyrite sample

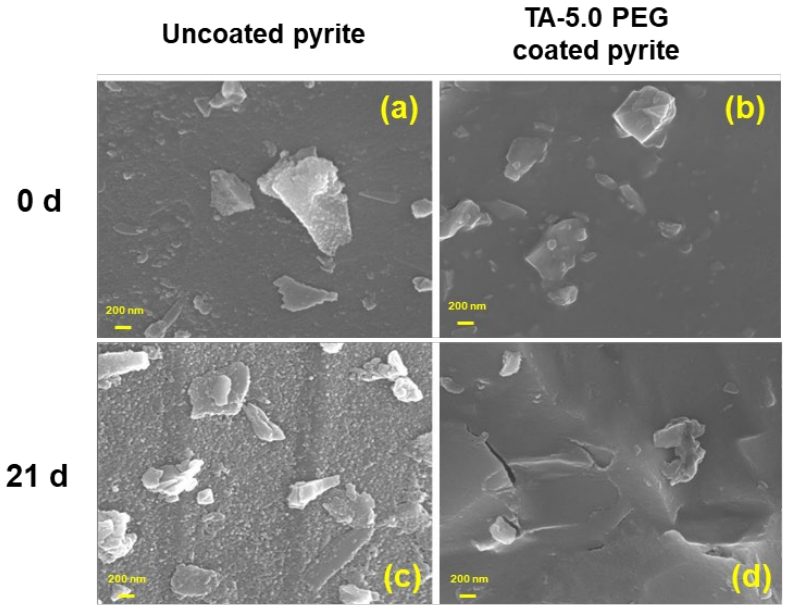


Figure S2. SEM images of uncoated pyrite (a, c) and TA-5.0 PEG coated pyrite (b, d) before and after a 21-day chemical leaching experiment.

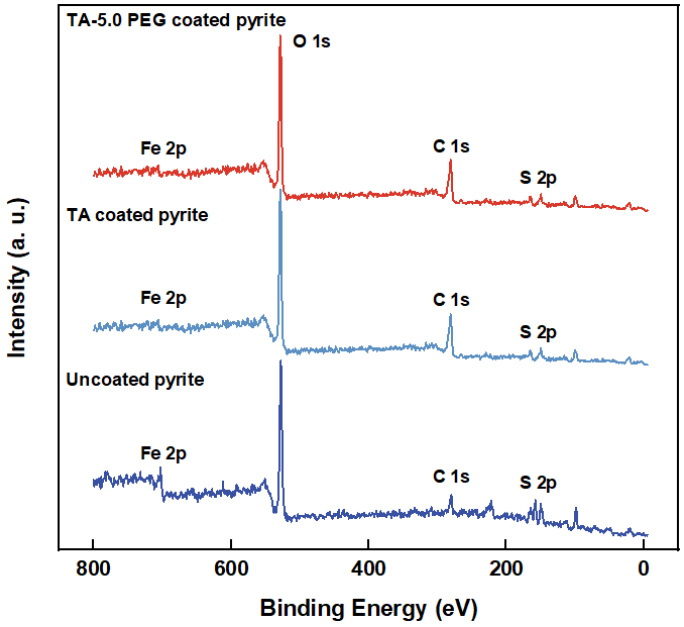


Figure S3. XPS survey spectra of uncoated, TA, and TA-5.0 PEG coated pyrite.

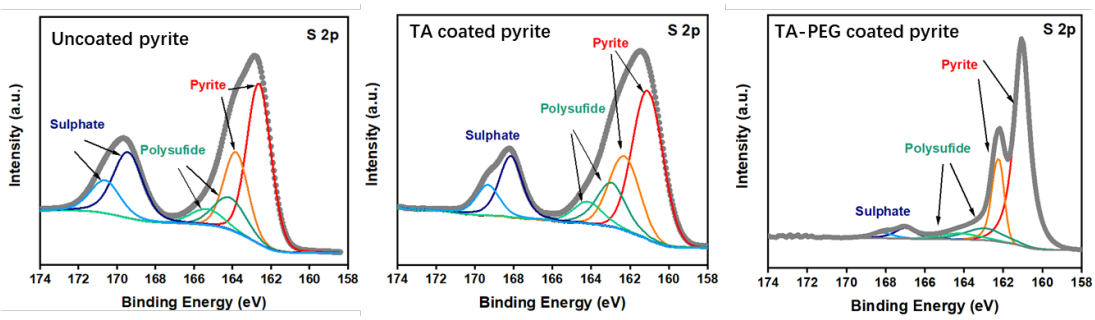


Figure S4. XPS devolution spectra of S 2p of uncoated, TA, and TA-5.0 PEG coated pyrite

Table S1. XPS fitting of C 1s, O 1s, Fe 2p, and S 2p of uncoated pyrite, TA, and TA-5.0 PEG coated pyrite.

Spectral Peak	Binding energy	FWHM	Chemical state	References
C 1s	284.32	1.88	C-C	(Chan-Rosado and Pech-Canul 2019, Li et al. 2023)
	283.52	2.13	C=C	(Wang et al. 2020)
	285.72	1.82	C-O	(Li et al. 2023)
	287.54	3.06	O-C=O	(Li et al. 2023)
O 1s	533.60	2.07	Si-O	(Li et al. 2023)
	531.10	1.87	Fe-O	(Li et al. 2023)
	532.65	1.80	Fe-OH	(Li et al. 2023)
	530.40	1.25	C-O	(Mei et al. 2015)

	529.45	1.48	C=O	(Geißler et al. 2016)
S 2p	170.65 169.45	1.49	Sulphate	(Primo et al. 2019)
	165.45 164.25	2.00	Polysulfide	(Primo et al. 2019)
	163.85 162.65	1.82	Pyrite	(Primo et al. 2019)
Fe 2p	712.20	2.40	Fe(III)	(Primo et al. 2019)
	710.15	2.40	Fe(II)	(Primo et al. 2019)
	714.10	2.30	Fe-O	(Primo et al. 2019)
	713.65	2.40	Fe-OH	(Li et al. 2023)
	715.95	2.40	Fe-S-O	(Li et al. 2023)
	707.40 720.40	2.59	Pyrite	(Primo et al. 2019)

References

Chan-Rosado, G. and Pech-Canul, M.A. (2019) Influence of native oxide film age on the passivation of carbon steel in neutral aqueous solutions with a dicarboxylic acid. Corrosion Science 153, 19-31.

Geißler, S., Barrantes, A., Tengvall, P., Messersmith, P.B. and Tiainen, H.J.L. (2016) Deposition kinetics of bioinspired phenolic coatings on titanium surfaces. Langmuir 32(32), 8050-8060.

Li, D., Chen, X., Liu, C., Tian, J., Li, F. and Liu, Y. (2023) Suppression of pyrite oxidation by co-depositing bio-inspired PropS-SH-tannic acid coatings for the source control acid mine drainage. Sci Total Environ 862, 160857.

Mei, L., Liao, L., Wang, Z. and Xu, C. (2015) Interactions between Phosphoric/Tannic Acid and Different Forms of FeOOH. Advances in Materials Science and Engineering 2015, 1-10.

Primo, E.N., Bracamonte, M.V., Luque, G.L., Bercoff, P.G., Leiva, E.P.M. and Barraco, D.E. (2019) Mechanochemically synthesized pyrite and its electrochemical behavior as cathode for lithium batteries. Journal of Solid State Electrochemistry 23(6), 1929-1938.

Wang, B., Moon, J.R., Ryu, S., Park, K.D. and Kim, J. (2020) Antibacterial 3D graphene composite gel with polyaspartamide and tannic acid containing in situ generated Ag nanoparticle. J Polymer Composites 41(7).